

Morpholino Monolayers: Preparation and Label-Free DNA Analysis by Surface Hybridization

****Supporting Information****

Napoleon Tercero^{1,2}, Kang Wang¹, Ping Gong², Rastislav Levicky^{1}*

¹Dept. of Chemical & Biological Engineering, Polytechnic Institute of New York University,
Brooklyn, NY 11201

²Dept. of Chemical Engineering, Columbia University, New York, NY 10027

S.1. Synthesis of Ferrocenecarboxylic Acid-NHS Ester (FC1) Tag. All reagents were obtained from Sigma-Aldrich and were used without purification. Molecular sieves were placed into tetrahydrofuran (THF) and methanol solvents to keep them free of moisture. The synthesis of FC1 followed closely the procedure reported by Takenaka and coworkers^{1,2} with modifications as per references 3 and 4. The following reagents were combined and stirred for 1 hr at 0 °C: 0.26 g (1.1 mmol; FW: 230.05, 97% purity) of ferrocene carboxylic acid in 4.8 ml THF, 0.14 g (1.2 mmol; MW: 115.10) of *N*-hydroxysuccinimide (NHS) in 4.8 ml THF, and 0.25 g (1.2 mmol; MW: 206.33, 99% purity) of dicyclohexylcarbodiimide (DCC) in 2.4 ml THF. The mixture was then kept at 4 °C for 48 hr. The precipitate (dicyclohexylurea) was filtered off using a fritted funnel. The filtrate was evaporated to dryness and the obtained solid product (FC1) was washed

with absolute methanol at 0 °C on a fritted funnel. After drying a 70% yield was obtained. The FC1 product was an orange-yellow powder as described in reference 3. ¹H NMR (300 MHz, DMSO, ppm): δ 2.515 (DMSO), 2.876 (s, 4H, -COCH₂-CH₂CO-), 3.337 (s, H₂O), 4.425 (s, 5H, Fc), 4.737 (t, 2H, Fc), 4.964 (t, 2H, Fc). Figure S1 shows the corresponding spectrum.

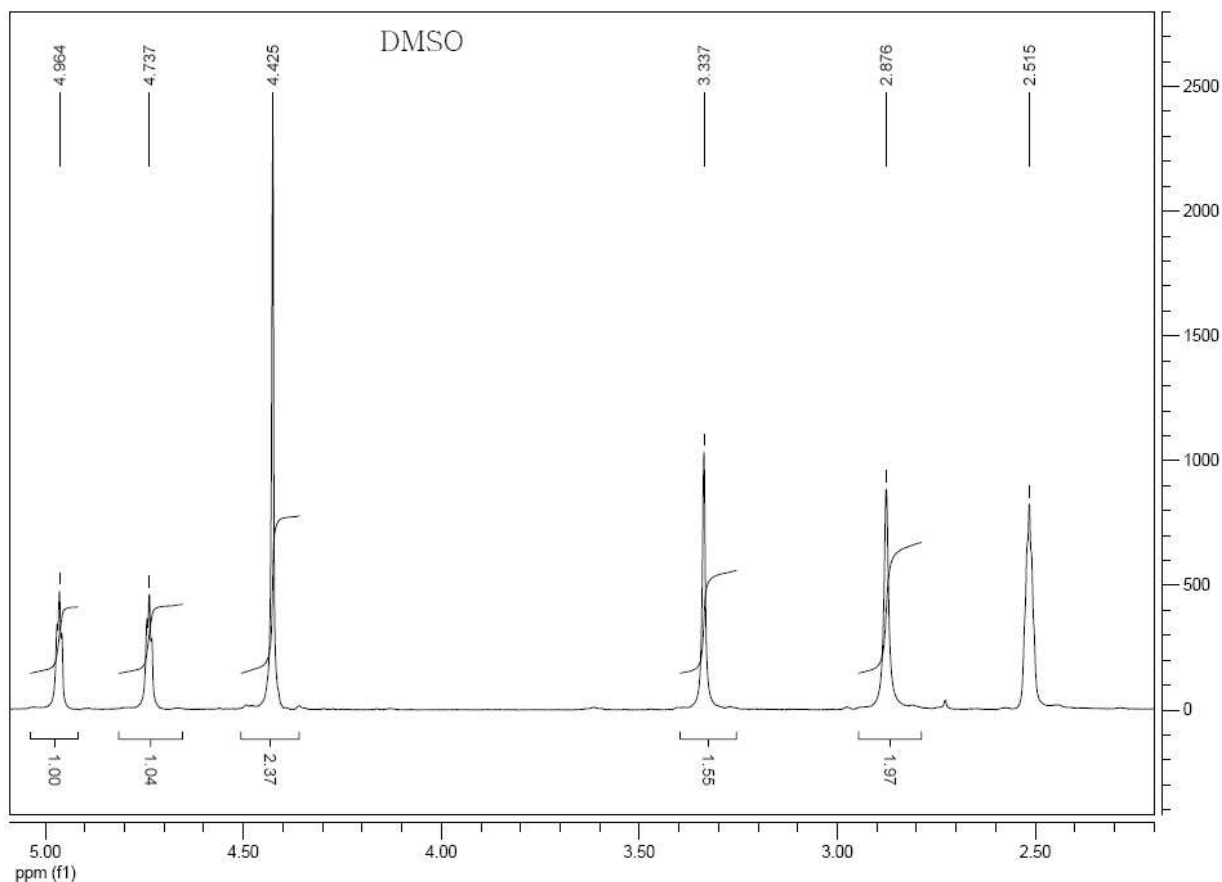


Figure S1. ¹H NMR spectrum of ferrocenecarboxylic acid-NHS ester product.

S.2. Bioconjugation of Ferrocene Tags. Probe and target oligomers were conjugated with FC1 and F2 tags as described in the manuscript, and as illustrated in Figure S2.

S.3. Fitting of Cyclic Voltammetry Data. The peak charges Q_{F2} and Q_{FC1} were determined by decomposing the experimentally measured current I_{EX} into its three components

$$I_{EX} = I_B + I_{T,F2} + I_{T,FC1} \quad (S1)$$

representing contributions from the baseline (I_B) and tag ($I_{T,F2}$; $I_{T,FC1}$) currents. The mathematical form of I_B was established empirically using monolayers of unlabeled probes – i.e. in the absence

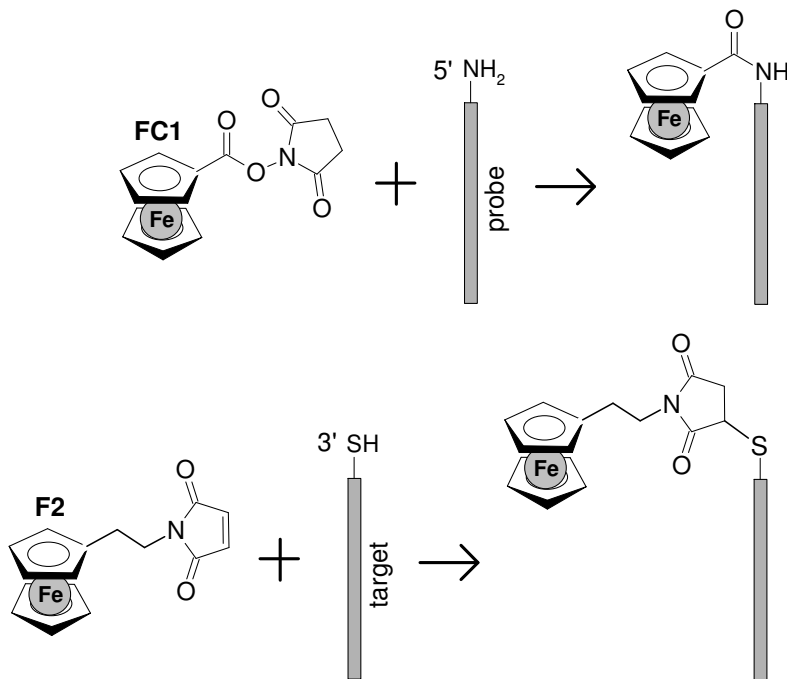


Figure S2. Top: Probe molecules were labeled with the electroactive tag FC1 using NHS ester to amine conjugation. **Bottom:** Target molecules were labeled with F2 via thiol-maleimide coupling.

of $I_{T,F2}$ and $I_{T,FC1}$ – and was found to be well captured by a combination of linear and stretched exponential functions,

$$I_B = a_1 + a_2 V + a_3 \exp(V^{a_4} / a_5) \quad (S2)$$

where V is the applied potential and a_1 through a_5 are adjustable parameters. The tag currents follow from theory⁵,

$$I_T = a_{6,T} \exp(a_{8,T}(V - a_{7,T})) / [1 + \exp(a_{8,T}(V - a_{7,T}))]^2 \quad (S3)$$

where $a_{7,T}$ is the tag's formal potential at the surface and $a_{6,T}$ and $a_{8,T}$ are parameters related to the peak area and width.

Probe and target coverages were calculated from the forward half of cyclic voltammograms. An initial guess for the baseline slope a_2 and the intercept a_1 was obtained from a cyclic voltammogram before hybridization - with only the probe FC1 peak present - using data between 0.1 V and 0.2 V where the probe tags do not contribute. The parameters a_1 and a_2 were then fixed and used in a fit of the first cyclic voltammogram that included both target and probe peaks, covering data from 0.1 V and up to the positive potential limit (typically 0.65 V). This fit yielded the additional baseline parameters a_3 , a_4 and a_5 , which were then held fixed for all subsequent cyclic voltammograms that tracked the growth of the target peak. The remaining six parameters $a_{6,i}$, $a_{7,i}$ and $a_{8,i}$ ($i = \text{FC1, F2}$) were fit for each successive trace to minimize the root-mean-squared error between the experimental and the calculated currents. The reason for excluding the first 0.1 V from fitting is that the model is not designed to capture the initial charging transient that occurs at the onset of a CV measurement. The numerical routine was implemented in FORTRAN. An initial optimization was carried out using the Nelder-Mead downhill simplex algorithm, followed by quasi-Newton optimization to more quickly converge to the error minimum.

S.4. Impact of Changes in Potential on Target Coverage. Measurement of a C_d - V_{DC} loop required 1 min to complete, during which time the surface bias was perturbed away from the hybridization potential of 0 V. Since changes in surface bias may be expected to have an impact on the extent of hybridization, there was concern that different parts of a C_d - V_{DC} loop could correspond to significantly different coverages of target molecules. This issue was addressed by performing hybridization controls with F2-labeled targets, using a sample with probe coverage of 7.0×10^{12} probes cm^{-2} and under 0.2 mol L^{-1} pH 7.0 sodium phosphate buffer. Control

experiments consisted of performing a CV measurement immediately before and after each C_d - V_{DC} loop to determine the pre- and post-execution target coverages. To minimize degradation of target F2 tags via the oxidized ferricinium form ^{6,7}, what would compromise accurate determination of coverage, V_{DC} was constrained to lie below the onset of F2 oxidation; i.e. not to exceed 0.05 V (note: all potentials are referenced to Ag/AgCl/3M NaCl). Thus, in the control experiments potential was looped between -0.2 V and 0.05 V, compared to between -0.2 V and 0.25 V for full C_d scans that used unlabeled targets.

Figure S3-A plots CV traces measured just before introduction of target at $t = 0$, and immediately before and after a C_d loop at $t = 6$ min and also at $t = 90$ min. In Figure S3-B, the target coverages determined from all the CV curves are plotted against time, both for measurements performed immediately before (filled points) and after (hollow points) a C_d loop. Changes in hybridization during execution of a C_d loop were modest; i.e. nearly the same extent of hybridization (within 10 %) was sampled by all points along a C_d - V_{DC} trace. In Figure S3-B a systematic, if slight, increase in target coverage is apparent for values determined from "after" CVs. While this increase may be a real effect, given the small differences it could also be an artifact brought on, for example, by variations in the CV baseline due to structural perturbation of the probe layer from stepping of the surface potential (during the C_d measurement). Such changes could subtly, and systematically, influence the CV fitting algorithm.

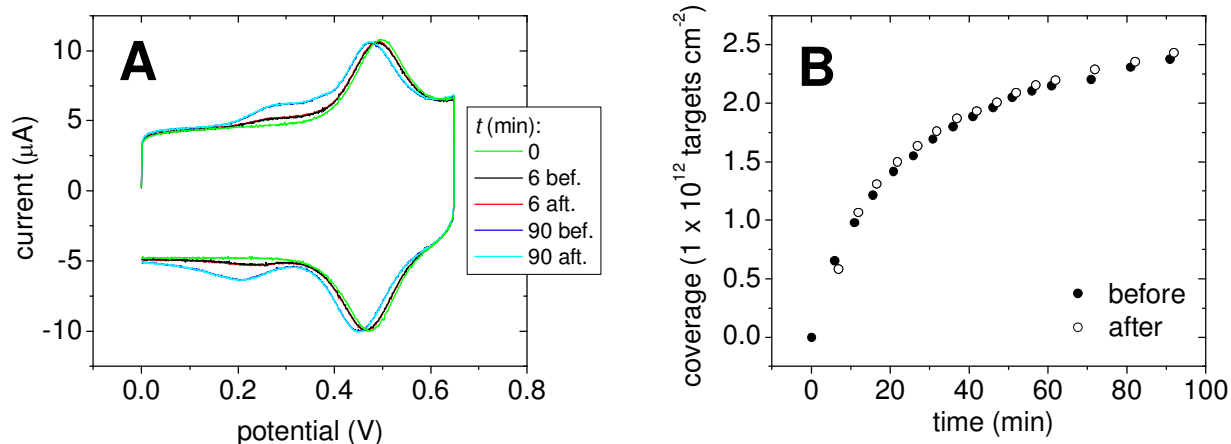


Figure S3. The impact of variation in surface potential V_{DC} on extent of hybridization during C_d measurement. Probe coverage: 7.0×10^{12} probes cm^{-2} . Buffer: 0.2 mol L^{-1} pH 7.0 sodium phosphate. **(A)** Sample CV traces. The $t = 0$ trace (green line) was taken immediately prior to addition of target, and shows only the Morpholino probe peak at 0.48 V. After 6 minutes of hybridization the "6 bef." voltammogram (black line) was measured, then an ac impedance C_d loop requiring 55 s to complete was carried out between -0.2 and 0.05 V with 0.025 V steps, followed by measurement of the "6 aft." voltammogram (red trace). A target peak starts to appear at around 0.25 V. A pair of "before" and "after" voltammograms is also shown after 90 minutes of hybridization. CV settings: 20 V s^{-1} between 0 and 0.65 V. **(B)** Corresponding target coverages determined by integration of target peaks from forward (anodic) half waves, from CVs determined immediately before (filled points) or after (hollow points) a C_d loop.

S.5. Nonspecific Binding Of Targets to Probes: CV Measurements. CV hybridization series, testing for sequence-nonspecific adsorption of TD2 targets to Morpholino PM1 probes, were carried out at conditions of 4.0×10^{12} probes cm^{-2} and 0.2 mol L^{-1} pH 7.0 sodium phosphate buffer. To provide a stricter test of nonspecific adsorption, a surface potential of 0.1 V, instead of

0 V, was used to facilitate adsorption of the negatively charged, noncomplementary TD2 targets. CV scans were obtained every 5 minutes at 20 V s^{-1} .

Figure S4 plots ten consecutive scans measured over 45 minutes in the presence of 25 nmol L^{-1} , F2-labeled TD2. A probe peak near 0.48 V is from the probes' FC1 tag. Presence of adsorbed targets would be signified by an F2 peak close to 0.25 V. The lack of F2 electroactivity indicates that noncomplementary binding was below the detection limit of $\sim 1 \times 10^{11}$ targets cm^{-2} . The low nonspecific adsorption was further confirmed by lack of response to addition of TD2 targets during label-free assays, as described in the main text.

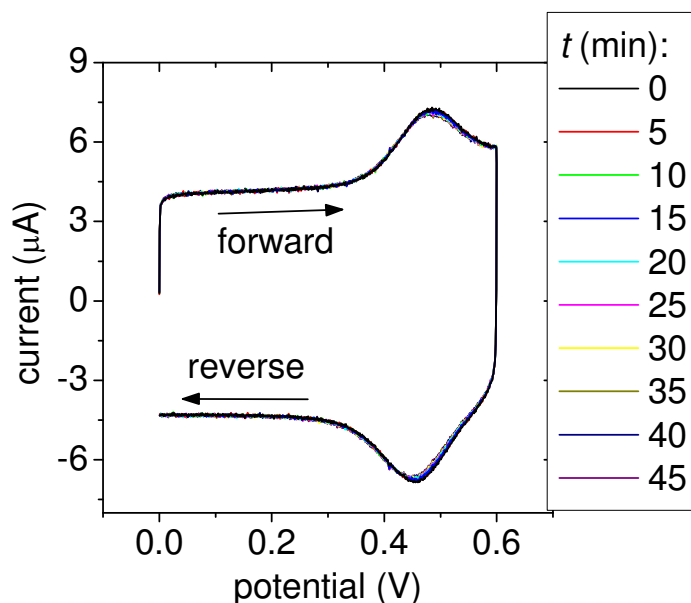


Figure S4. Ten consecutive CV voltammograms, measured over 45 minutes, in the presence of 25 nmol L^{-1} of F2-labeled TD2 target. Conditions: 4.0×10^{12} probes cm^{-2} , 0.2 mol L^{-1} pH 7.0 sodium phosphate, 0.1 V surface bias.

References for Supporting Information

- (1) Takenaka, S.; Uto, Y.; Kondo, H.; Ihara, T.; Takagi, M. *Anal. Biochem.* **1994**, *218*, 436-443.
- (2) Ihara, T.; Maruo, Y.; Takenaka, S.; Takagi, M. *Nucl. Acids. Res.* **1996**, *24*, 4273-4280.
- (3) Brazill, S. A.; Kim, P. H.; Kuhr, W. G. *Anal. Chem.* **2001**, *73*, 4882-4890.
- (4) Kutner, A.; Renstrom, B.; Schnoes, H. K.; DeLuca, H. F. *Proc. Natl. Acad. Sci. USA* **1986**, *83*, 6781-6784.
- (5) Laviron, E. *J. Electroanal. Chem.* **1979**, *100*, 263-270.
- (6) Popenoe, D. D.; Deinhammer, R. S.; Porter, M. D. *Langmuir* **1992**, *8*, 2521-2530.
- (7) Prins, R.; Korswagen, A. R.; Kortbeek, A. G. T. G. *J. Organomet. Chem.* **1972**, *39*, 335-344.

Full Citations for References with More Than 15 Authors:

reference 30:

Hughes, T. R.; Mao, M.; Jones, A. R.; Burchard, J.; Marton, M. J.; Shannon, K. W.; Lefkowitz, S. M.; Ziman, M.; Schelter, J. M.; Meyer, M. R.; Kobayashi, S.; Davis, C.; Dai, H.; He, Y. D.; Stephanians, S. B.; Cavet, G.; Walker, W. L.; West, A.; Coffey, E.; Shoemaker, D. D.; Stoughton, R.; Blanchard, A. P.; Friend, S. H.; Linsley, P. S. *Nat. Biotechnol.* **2001**, *19*, 342-347.